Developmental Cognitive Neuroscience 47 (2021) 100881

Contents lists available at ScienceDirect

Developmental Cognitive Neuroscience

journal homepage: www.elsevier.com/locate/dcn

White-matter tract connecting anterior insula to nucleus accumbens predicts greater future motivation in adolescents

Josiah K. Leong [a,b,*], Tiffany C. Ho [c,d], Natalie L. Colich [e], Lucinda Sisk [f], Brian Knutson [c,g], Ian H. Gotlib [c,g]

[a] University of Arkansas, Department of Psychological Science, Fayetteville, AR, United States
[b] Indiana University, Department of Psychological and Brain Sciences, Bloomington, IN, United States
[c] Stanford University, Department of Psychology, Stanford, CA, United States
[d] University of California, San Francisco, Department of Psychology & Weill Institute for Neurosciences, San Francisco, CA, United States
[e] University of Washington, Department of Psychology, Seattle, WA, United States
[f] Yale University, Department of Psychology, New Haven, CT, United States
[g] Stanford University, Wu Tsai Neurosciences Institute, Stanford, CA, United States

ARTICLE INFO

Keywords:
White matter
Nucleus accumbens
Anterior insula
Multimodal neuroimaging
Monetary incentive delay task
Reward

ABSTRACT

The motivation to approach or avoid incentives can change during adolescence. Advances in neuroimaging allow researchers to characterize specific brain circuits that underlie these developmental changes. Whereas activity in the nucleus accumbens (NAcc) can predict approach toward incentive gain, activity in anterior insula (AIns) is associated with avoidance of incentive loss. Recent research characterized the structural white-matter tract connecting the two brain regions, but the tract has neither been characterized in adolescence nor linked to functional activity during incentive anticipation. In this study, we collected diffusion MRI and characterized the tract connecting the AIns to the NAcc for the first time in early adolescents. We then measured NAcc functional activity during a monetary incentive delay task and found that structural coherence of the AIns-NAcc tract is correlated with decreased functional activity at the NAcc terminal of the tract during anticipation of no incentives. In adolescents who completed an assessment 2 years later, we found that AIns-NAcc tract coherence could predict greater future self-reported motivation, and that NAcc functional activity could statistically mediate this association. Together, the findings establish links from brain structure to function to future motivation and provide targets to study the reciprocal development of brain structure and function.

1. Introduction

Adolescence is a period of human development marked by increased sensitivity to rewards (Spear, 2000; Steinberg et al., 2009). Compared to both children and adults, adolescents exhibit increased approach behaviors, novelty seeking, and risk taking (Spear, 2000; Sisk and Foster, 2004; Steinberg, 2009). Whereas increased reward sensitivity and motivated behavior can promote healthy development by facilitating learning and improving adaptation to new environments (Davidow et al., 2016; Telzer, 2016), these same behavioral shifts may also partially account for the higher rate of vehicle accidents, drug abuse, and unsafe sex practices in adolescents compared to adults (Eaton et al., 2012; Substance Abuse and Mental Health Services Administration (SAMHSA, 2012). Given the significant societal costs of these behaviors, researchers have attempted to understand characteristics of the adolescent brain that promote and restrain the pursuit of rewards (Dahl et al., 2018; Foulkes and Blakemore, 2018; Casey et al., 2018), with the goal of identifying neural targets to strategically increase self-control of motivated behaviors.

Converging evidence across mammalian species suggests that dopaminergic projections from the ventral tegmental area to the nucleus accumbens (NAcc) can drive behaviors related to the anticipation and consumption of both primary (e.g., food) and secondary (e.g., money) incentives (Ikemoto and Panksepp, 1999). Countervailing projections from the prefrontal cortex (PFC) and the anterior insula (AIns) release the neurotransmitter glutamate into the NAcc and may inhibit neural responses to reward (Ferenczi et al., 2016). Human functional neuroimaging research indicates that greater anticipatory activity in the NAcc

* Corresponding author at: 216 Memorial Hall, Fayetteville, AR, 72701, United States.
E-mail address: josiah@uark.edu (J.K. Leong).

https://doi.org/10.1016/j.dcn.2020.100881
Received 29 April 2020; Received in revised form 22 September 2020; Accepted 3 November 2020
Available online 10 November 2020

predicts risk-seeking choices, whereas greater anticipatory activity in the AIns predicts risk-averse choices in a financial investment task (Kuhnen and Knutson, 2005). In particular, positively skewed gambles, which offer a low probability of high magnitude rewards, can preferentially increase NAcc activity (Wu et al., 2011; Leong et al., 2016). Activity in the AIns may counter the risk-seeking signals in the NAcc, since lesions of the AIns are associated with increased financial risk taking (Clark et al., 2014) and impaired associative learning from losses but not from gains (Palminteri et al., 2012). Thus, whereas NAcc activity is posited to index positive arousal and promote approach behavior, AIns activity appears to index negative arousal and promote avoidance behavior (Knutson et al., 2014). The comparative and functional neuroimaging research suggests that a structural tract connecting the AIns to the NAcc might be related to decreased NAcc activity and risk-seeking behavior.

Recent multimodal neuroimaging research has combined diffusion MRI and probabilistic tractography to characterize the structural connection between the AIns and the NAcc. Specifically, Leong et al. (2016) visualized and measured a white-matter tract connecting the AIns to the NAcc in adults and found that greater AIns-NAcc tract coherence, indexed by higher fractional anisotropy (FA) values, is associated with reduced preference for positively skewed gambles. Leong et al. also found that lower activity in the NAcc prior to gamble choice, measured by functional MRI (FMRI), statistically mediated the association between AIns-NAcc tract coherence and positive-skew gambling behavior. Physiological research helped guide the interpretation of these results, which suggest that unidirectional glutamatergic projections from the AIns to the NAcc blunts NAcc responses to potential incentives, thereby reducing risky choices (Chikama et al., 1997; Reynolds and Zahm, 2005; Ferenczi et al., 2016). The studies suggest a circuit model of reward processing in which the NAcc responds to potential rewards, the AIns responds to aversive signals (Knutson and Bossaerts, 2007; Craig, 2009), and together influence the flow of activity through corticostriatal loops that can incite or inhibit motivated behaviors (Haber and Knutson, 2010; Samanez-Larkin and Knutson, 2015).

Whereas the previous multimodal neuroimaging explorations of the AIns-NAcc circuit were conducted in adults, adolescence is a period of human development when the NAcc and the AIns undergo significant functional and structural changes. Functionally, previous research has shown that NAcc activity in response to gain outcomes peaks around age 15 and decreases with age (Braams et al., 2015; Schreuders et al., 2018; Insel and Somerville, 2018). In contrast, AIns activity dips to a nadir around 17 years of age and increases with age (Insel and Somerville, 2018). Structurally, coherence of white matter within the right-hemisphere insula is positively correlated with the onset of puberty (Herting et al., 2012), and structural coherence increases from adolescence to adulthood in the uncinate fasciculus — a major tract that passes through the white matter adjacent to the insula (Lebel et al., 2008; Simmonds et al., 2014). These findings identify adolescence as a period during which the NAcc and AIns functionally respond to incentives in distinct ways, and further indicate that greater NAcc activity and lesser AIns activity may relate to increased risk taking. The early research suggests that the changes in NAcc and AIns functional activity may occur in concert with structural changes to the white-matter connections between the two brain regions.

While researchers have documented significant functional changes in the NAcc and the AIns during adolescence, no studies have examined the white-matter tract connecting the two brain regions during this developmental period. Further, no studies of adolescents have combined measures of AIns-NAcc tract coherence with measures of functional activity in the projection targets of the tract during incentive anticipation. Establishing a link between structural tract coherence and functional activity can guide novel hypotheses about the temporal or causal nature of the relation between structural development and circuit function. The reliable measurement of both the structure and function of the AIns-NAcc circuit may help to explain individual differences in personality, however no study has linked multimodal measurements of the AIns-NAcc circuit to individual differences in personality.

In this study, we innovated multimodal neuroimaging analyses to characterize the AIns-NAcc white-matter tract and to test links between the structural coherence of the tract to functional NAcc activity in 91 early adolescents (ages 9–13 years; Tanner stage $\leq$ 3). We collected diffusion MRI and conducted probabilistic tractography to trace the AIns-NAcc tract in every individual. We then measured whole-brain FMRI activity in response to gains and losses during a monetary incentive delay task. Given evidence from animal studies that unidirectional glutamatergic axons from the AIns terminate in the NAcc (Chikama et al., 1997; Reynolds and Zahm, 2005), we hypothesized that coherence of the AIns-NAcc tract is negatively associated with NAcc activity during the task (see also Leong et al., 2016). Specifically, we tested whether AIns-NAcc tract coherence was associated with functional NAcc activity during the anticipation of incentives (gains, losses, and no incentive). Finally, in a subset of 69 participants who were assessed two years later, we tested whether AIns-NAcc tract coherence at baseline could predict future self-reported reward drive and impulsivity, and whether functional NAcc activity could statistically mediate the association between AIns-NAcc tract coherence and future reward motivation.

2. Materials and methods

2.1. Participants and procedures

Participants were native English speakers from the San Francisco Bay Area who were recruited by media and online advertisements for a longitudinal study of adolescent brain development (see King et al., 2017, and Colich et al., 2017, for additional details about participant recruitment). Given the focus of the larger study on pubertal development, females were excluded from the study if they had experienced the onset of menses at entry to the study, and participants with an average Tanner score above 3 were excluded. Males and females were matched on self-reported pubertal stage (Morris and Udry, 1980). Participants were excluded from the study if they had any contraindications for MRI (e.g., had metal implants, braces), had a history of neurological disorder or major medical illness, had cognitive or physical challenges that limited their ability to understand or complete the study procedures, or were not fluent in English. Of 182 total study participants who attempted an MRI scan, 159 successfully completed both functional and diffusion MRI scans at baseline, and 99 participants remained after quality control (excluded 33 participants for motion $>$ 2 mm between volume acquisitions in any direction for functional scans; excluded 27 participants for motion $>$ 5 mm on average in any direction across the diffusion scan). An additional 8 participants were excluded for lack of engagement in the task ($<$ 30 % hit rate), leaving a total of 91 participants (see Table 1 for participant demographics). A subset of participants (n = 69) completed a behavioral session approximately 24 months after the baseline time point (mean = 23.4 months; SD = 5.0 months;

Table 1
Participant Demographic Characteristics.

Item	
N (Baseline)	91 (32 male)
N (Follow-Up)	69 (25 male)
Baseline Age (Years)	11.38 ± 1.03 (9–13)
Baseline Tanner Stage	1.96 ± 0.66 (1–3)
Interval between Baseline and Follow-Up (Months)	23.41 ± 4.96 (16.95–39.56)
Race/Ethnicity	
White	50.55 %
Asian	15.48 %
African American	9.89 %
Hispanic	5.49 %
Biracial	9.89 %
Other	6.59 %
Unknown	1.10 %

range = 17.0–39.6 months). The study was approved by the Stanford University Institutional Review Board. In accordance with the Declaration of Helsinki, all participants provided informed assent and their parent/legal guardian provided informed consent.

2.2. Pubertal stage

Pubertal stage was determined by self-report Tanner Staging (Marshall and Tanner, 1969; Morris and Udry, 1980). Participants reported her/his developmental stage by selecting from a schematic drawing of two secondary sex characteristics (pubic hair and breast/-testes development) on a scale of 1–5. Self-report Tanner staging scores are correlated with physicians' physical examinations of pubertal development (Shirtcliff et al., 2009; Coleman and Coleman, 2002).

2.3. MRI scan acquisition

MRI scans were acquired at the Center for Cognitive and Neurobiological Imaging (CNI) at Stanford University using a 3 T Discovery MR750 (GE Medical Systems, Milwaukee, WI) equipped with a 32-channel head coil (Nova Medical). Whole-brain functional scans were acquired during the KIDMID task (see below for more details) with a T2*-weighted gradient pulse sequence (46 axial slices, TR/TE = 2000/24 ms, flip angle = 77°, 2.9 mm isotropic voxels, interleaved acquisition). Diffusion-weighted imaging was acquired to visualize and measure structural white-matter tracts (TR/TE = 8500/93.5 ms, 64 axial slices, 2 mm isotropic voxels, 60 b = 2000 diffusion-weighted directions, and 6 b = 0 acquisitions at the beginning of the scan). A high-resolution T1-weighted anatomical scan was acquired for co-registration of functional images and diffusion data and for volume of interest specification with a SPGR sequence (TR/TE/TI = 6.24/2.34/450 ms; flip angle = 12°; sagittal slices; 0.9 mm isotropic voxels).

2.4. Kid monetary incentive delay (KIDMID) task

The Monetary Incentive Delay (MID) task reliably elicits FMRI activity in mesolimbic brain circuits in healthy adults (Knutson et al., 2001). We modified the MID task for children (KIDMID) by replacing the monetary incentive with points, which participants could later exchange for prizes they had selected before starting the task (Gotlib et al., 2010). Participants completed 72 pseudo-randomized trials (see Fig. 1). On every trial, participants viewed an incentive cue (500 ms), anticipated the incentive (2000–2500 ms), responded to the target (160–350 ms, adaptive timing), fixated for a delay (900–1500 ms), and viewed the trial outcome (1500 ms). Participants were asked to respond to the target (a triangle) as quickly as possible; they were successful if they responded before the target disappeared. Each trial lasted 6000 ms and was locked to three FMRI volume acquisitions (TR = 2000 ms). Cues indicated 4 incentive conditions: gain (+5 points), non-gain (+0), loss (-5), and non-loss (-0). Circles indicated gain trials and squares indicated loss trials. In loss trials, participants had to respond to the target in order to avoid losing points. Following the task, participants exchanged the total points they had earned in the task for prizes. The reaction time required to successfully hit the target was dynamically adjusted by a staircase procedure to keep each participant's hit rate at 66 % across all conditions.

2.5. Functional MRI preprocessing and analysis

Functional neuroimaging analyses were conducted with Analysis of Functional NeuroImages (AFNI) software (Cox, 1996). For preprocessing, data were sinc interpolated to correct for non-simultaneous slice acquisition, corrected for motion in six dimensions, spatially smoothed using a small kernel (full width at half maximum = 4 mm), and high-pass filtered (omitting frequencies with period slower than 90 s). Visual inspection of motion correction estimates confirmed that six participants' heads had moved more than 2 mm in a plane from one whole-brain volume acquisition to the next; these participants were excluded from further analysis.

Whole-brain statistical analyses were conducted with regression models that included eleven regressors of no interest that included: (1) six regressors that indexed motion across volume acquisitions; (2) two

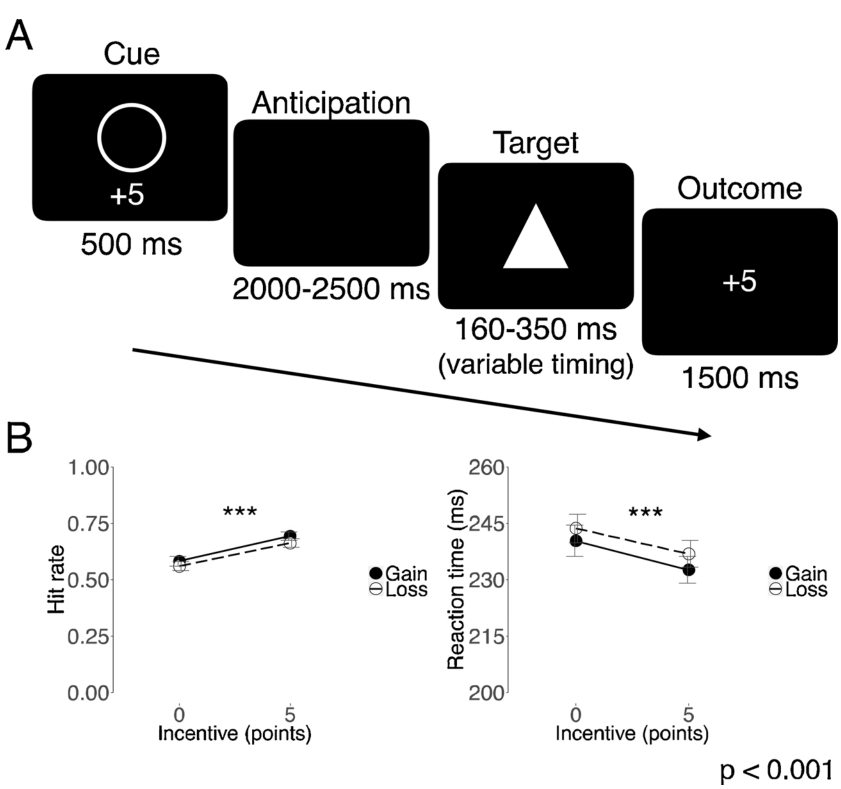

Fig. 1. Kid Monetary Incentive Delay (KIDMID) task trial structure and behavior.
(A) The Monetary Incentive Delay task for children (KIDMID) has 72 pseudo-randomized trials with 4 conditions: gain (+5 points), non-gain (+0), loss (-5), and non-loss (-0). In every trial, participants viewed an incentive cue (500 ms), anticipated the incentive (2000–2500 ms), responded to the target (160–350 ms, variable timing), fixated for a delay (900–1500 ms), and viewed the trial outcome (1500 ms). Trials lasted 6000 ms and were locked to three FMRI volume acquisitions (TR = 2000 ms).
(B) Participants hit more targets on gain versus non-gain trials (paired $t(90) = 5.36$, $p < 0.001$), and on loss versus non-loss trials (paired $t(90) = 5.62$, $p < 0.001$). Participants had faster reaction times for gain than non-gain trials (paired $t(90)=-2.29$, $p = 0.02$), and were faster in avoiding losses than avoiding non-losses (paired $t(90)=-3.32$, $p < 0.01$).

regressors that indexed activity in cerebrospinal fluid and white matter volumes of non-interest; and (3) three regressors that indexed the anticipation, target, and outcome periods across all trials. Four orthogonal regressors of interest contrasted: (1) gain versus non-gain anticipation; (2) loss versus non-loss anticipation; (3) gain versus non-gain outcome; and (4) non-loss versus loss outcome. These orthogonal regressors of interest were convolved with a single gamma-variate function that modeled the canonical hemodynamic response (Cohen, 1997) before inclusion in the regression model.

For group statistical maps, each participant's t-statistic map of regressors of interest was transformed to Z-scores, spatially warped to Talairach space, and resampled to 2 mm cubic voxels. Group maps were voxelwise thresholded ($p < 0.001$) and then cluster thresholded (cluster size > 12 contiguous 2.9 mm cubic voxels) to yield a corrected threshold for detecting activity within a gray matter mask ($p < 0.05$ corrected, derived with 10,000 Monte Carlo iterations using the program 3dClustSim (AFNI_18.0.25 version), which estimates the spatial autocorrelation of noise to minimize false positive findings (Cox et al., 2017).

To extract raw activity for targeted volume-of-interest (VOI) analyses, spheres (8 mm diameter) were centered on bilateral foci for the NAcc and the AIns (Talairach coordinates: +/-10, 12, -2; +/-34, 24, -4; Knutson and Greer, 2008). VOIs were warped from Talairach space to participants' native brain space. Activity was averaged within the VOI and then divided by the mean VOI activity across the whole experiment to derive a continuous measure of percent signal change. Activity time courses were then shifted 2 volume acquisitions (or 4 s) to account for the hemodynamic response lag to peak response. Percent signal change was extracted from the trial periods when participants viewed and anticipated incentive cues (i.e., the first volume acquisition), responded to the target in each trial (second volume acquisition), and viewed the trial outcome (third volume acquisition). The mean activity in the VOIs during these periods was used in between-subject analyses. Brain activity in any VOI that was greater than 4 standard deviations from the mean percent signal change in that VOI was excluded from regression models. Statistical analyses were performed in R (version 3.4.0), using packages for mixed effects regression analysis (lme4 version 1.1–15) and statistical mediation analysis (lavaan version 0.5–23.1097).

2.6. Diffusion MRI preprocessing

Anatomical landmarks were manually defined in the anterior and posterior commissures (AC-PC), and the midsagittal plane to guide a rigid-body transformation that converted the T1-weighted images into AC-PC aligned space. Participant motion in the diffusion-weighted images was corrected by non-linear co-registration. Each diffusion-weighted image was registered to the mean of the six motion-corrected non-diffusion-weighted ($b = 0$) images. The mean of the six non-diffusion-weighted images was aligned to the T1 image in AC-PC space using a rigid body transformation. All raw diffusion images were resampled to 2 mm isotropic voxels by combining motion correction and anatomical alignment into one transformation, and then resampling the data using a seventh-order b-spline algorithm. All preprocessing steps were performed using the open-source mrDiffusion package (www.github.com/vistalab/vistasoft).

2.7. Probabilistic tractography of the AIns-NAcc tract

To define anatomical VOIs, each participant's AC-PC aligned T1-weighted image was processed through FreeSurfer (version 5.3), an automated cortical parcellation and subcortical segmentation software suite (Fischl et al., 2004; Fischl, 2012). AIns VOIs were derived from the Destrieux cortical parcellation atlas, by combining the anterior insula and short gyrus parcellations (Destrieux et al., 2010; Leong et al., 2016). NAcc VOIs were identified from probabilistic subcortical tissue classification based on a manually labeled training set (Desikan et al., 2006). A binary white-matter mask was formed using the white versus gray-matter border identified by FreeSurfer. The FreeSurfer VOIs were visually inspected for each individual to ensure that they covered the relevant brain regions, and were processed to fill holes in the VOI and remove satellite voxels, and then dilated 1 voxel along the VOI border. This additional processing of the VOIs helped to prevent circular tracking (i.e., tracking fibers within the VOI), and ensured that fibers successfully left the VOI (i.e., exited the gray matter and entered the white matter).

Fiber tracking between the AIns and NAcc VOIs was performed using constrained spherical deconvolution-based probabilistic tracking, sometimes called probabilistic streamline tractography, as implemented in MRtrix software (version 0.2.12; Tournier et al., 2007) and has been previously described (Leong et al., 2016, 2018). The maximum number of harmonics was set to 6 ($L_{max} = 6$), which defined the maximum number of deconvolution kernels utilized by constrained spherical deconvolution to estimate the fiber orientation distribution function in each voxel. This required 28 parameters for fitting the function (or 32 less than the 60 measured diffusion directions). Fiber pathways were generated by randomly seeding a voxel in a starting VOI and tracking until the fiber reached the ending VOI to ensure symmetrical fiber tracking (maximum number of fibers = 5000, FA cutoff = 0.1, curvature = 60 degrees). Fibers leaving the white-matter mask were terminated and discarded.

Fibers obtained from the tractography solutions were then reduced to core fiber bundles by eliminating outliers and anatomically unlikely pathways (e.g., fibers crossing the cerebral hemispheres, or crossing through cerebrospinal fluid). Specifically, fibers longer or shorter than 2 standard deviations from the mean fiber length were initially removed. Next, fibers greater than 3 standard deviations away from the mean spatial position of the core fiber (Mahalanobis distance) were removed. Finally, fibers that took indirect routes between VOIs (e.g., fibers that projected in one direction but then looped backward) were removed.

2.8. Structural coherence of the AIns-NAcc tract

After identifying the AIns-NAcc tract in all participants, we quantified measures of the structural coherence of the tract in both hemispheres. The structural coherence of a tract can be estimated with diffusion metrics such as mean FA. To assess FA along the spatial trajectory of the tract, we spatially normalized fiber pathways between participants by sampling 100 evenly-spaced cross-sectional nodes along the length of the tract from the start VOI to the end VOI (Yeatman et al., 2012; Ho et al., 2017). The mean FA in each node of the tract was then calculated by averaging FA from all fibers within a node, weighted by the spatial distance of a fiber from the node's core fiber. We calculated structural coherence of the tract by averaging FA across the middle 50 % of the tract to ensure that coherence measures exclusively included white matter and not voxels along the gray versus white-matter boundary. Indexing structural coherence in the middle half of each tract follows previous tractography methods, and can also minimize the influence of branching fibers near the tract ends (Yeatman et al., 2012). This procedure generated a single FA value for the tract in each hemisphere of every participant, and provided the estimate of structural tract coherence. The instructions and open-source code for these procedures are available on GitHub (https://github.com/josiahkl/spantracts).

2.9. Sensitivity to punishment and sensitivity to reward questionnaire for children (SPSRQ-C)

All participants completed a 29-item self-report questionnaire adopted from the SPSRQ-C (Colder et al., 2011) at both timepoints. The questionnaire yields scores for five subscales: drive, impulsivity/fun, social approval, fear, and, anxiety. Participants responded to questions on a Likert scale, ranging from 1 (“strongly disagree”) to 5 (“strongly agree”). Subscale scores were calculated by averaging participant responses across the items comprising each subscale.

Recent research in human personality has adapted adult self-report tests of the behavioral approach and inhibition system (BAS and BIS) for assessment in children (Torrubia et al., 2001), specifically, the Sensitivity to Punishment and Sensitivity to Reward Questionnaire (SPSRQ-C; Colder and O'Connor, 2004). While factor analysis of the SPSRQ-C distinguises separate factors for "drive" and "impulsivity or fun seeking," both factors contain questions regarding sensation seeking and risk taking (Colder et al., 2011). Thus, we tested whether coherence of the AIns-NAcc structural tract might be related to SPSRQ-C drive and impulsivity scores.

3. Results

3.1. Behavioral performance on the KIDMID task

Participants hit more targets on incentivized than on non-incentivized trials in the KIDMID task (gain versus non-gain: paired $t(90) = 5.36$, $p < 0.001$; loss versus non-loss: paired $t(90) = 5.62$, $p < 0.001$; see Fig. 1). This better performance for incentivized trials was reflected in faster reaction times for incentivized than for non-incentivized trials (gain versus non-gain: paired $t(90)$=-2.29, $p = 0.02$; loss versus non-loss: paired $t(90)$=-3.32, $p < 0.01$). Replicating prior research, faster reaction times were associated with increased self-report drive and impulsivity on the SPSRQ-C questionnaire at baseline (r=-0.29, $p < 0.01$; see Supplementary Fig. 1; Colder et al., 2011).

3.2. Whole-brain and VOI activity in the KIDMID task

As in previous research, whole-brain FMRI analyses revealed increased mesolimbic activity during anticipation of potential gains versus non-gains (see Fig. 2). Analyses also revealed increased medial PFC activity during receipt of gains and increased left AIns and right ventrolateral PFC activity during receipt of non-gains (see Fig. 2). Raw NAcc VOI activity was greater during anticipation of incentives than

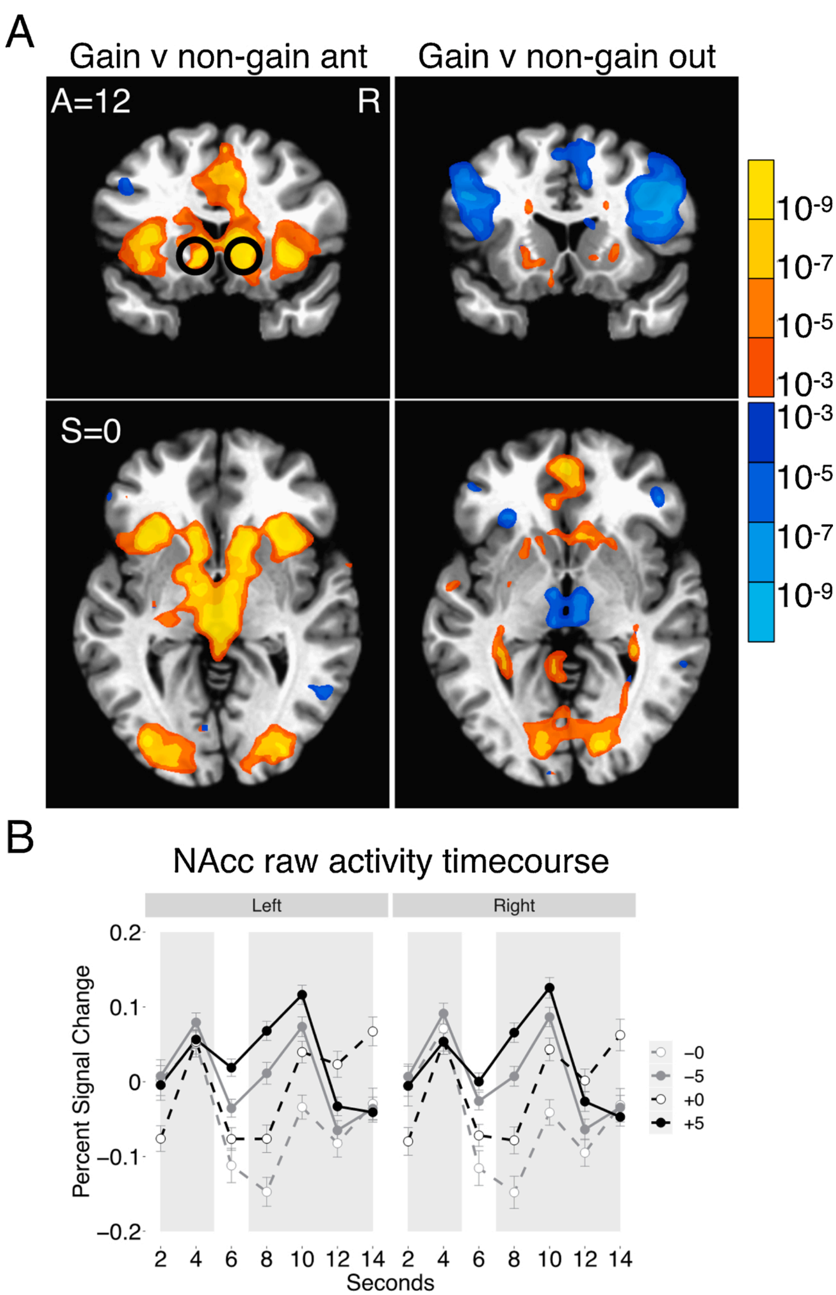

Fig. 2. Functional MRI whole-brain contrasts and NAcc raw activity timecourses.
(A) Whole-brain FMRI analyses revealed increased mesolimbic activity during anticipation of potential gains versus non-gains (voxelwise $p < 0.001$, cluster-corrected $p < 0.05$). There was increased medial PFC activity during receipt of gains, and increased left anterior insula and right ventrolateral PFC activity during receipt of non-gains. The spherical NAcc VOI indicates where raw activity was extracted for time course and individual difference analyses. See Supplementary Fig. 2 for equivalent whole-brain maps of the loss and non-loss conditions.
(B) Raw percent signal change in NAcc activity was plotted to illustrate critical predictions. In both hemispheres, NAcc activity was greater when anticipating potential gains than non-gains (gain versus non-gain: paired $t(90) = 4.46$, $p < 0.001$), and when anticipating potential losses than non-losses (paired $t(90) = 3.24$, $p < 0.01$). NAcc activity was additionally greater during the anticipation of gains than the anticipation of losses (paired $t(90)$=-2.76, $p < 0.01$).

non-incentives (gain versus non-gain: paired $t(90) = 4.46$, $p < 0.001$; loss versus non-loss: paired $t(90) = 3.24$, $p < 0.01$). Mean NAcc activity during anticipation of each incentive (i.e., the first volume acquisition in the trial lagged by two volumes, or 4 s) was computed for each participant and then used in analyses examining individual differences.

3.3. Structural tract coherence

Probabilistic tractography revealed the AIns-NAcc tract in both hemispheres in every participant (see Fig. 3). Tractography results reproduced an AIns-NAcc tract trajectory in adolescents similar to that previously visualized in adults (Leong et al., 2016, 2018). FA along the middle 50 % of the tract was averaged in each hemisphere to derive a measure of tract coherence in each participant. Because animal tract tracings indicate that unidirectional axons from the AIns terminate in the NAcc (Chikama et al., 1997; Reynolds and Zahm, 2005), we tested the hypothesis that coherence of the AIns-NAcc tract was associated with NAcc activity during the anticipation phase of the MID task.

Individual differences in AIns-NAcc tract coherence (FA) was associated with decreased NAcc activity when participants anticipated non-gains (see Fig. 4; right: β=-0.28, $t(89)$=-2.70, $p < 0.01$; left: β=-0.21, $t(89)$=-2.02, $p < 0.05$). Bootstrapped correlations demonstrated the robustness of this association in the right hemisphere (samples=10,000; right: 95 % confidence interval = [-0.45, -0.03], $p = 0.02$; left: 95 % confidence interval = [-0.43, -0.01], $p = 0.09$). A non-parametric Spearman's correlation also confirmed the robustness of the association in both hemispheres (95 % confidence interval: [-0.39, -0.003]). Given the potential concern about using spherical versus atlas VOIs, we reproduced the findings when extracting NAcc activity from a probabilistic VOI derived from the Desai atlas (right: β=-0.32, t(89)=-3.19, p<0.01; left: β=-0.17, t(89)=-1.64, p=0.10). Tract coherence was not associated with NAcc activity when participants anticipated gains (right: β=0.05, $t(89) = 0.50$, $p = 0.62$; left: β=0.02, $t(89) = 0.19$, $p = 0.85$).

Additional statistical analyses tested the potential association between tract coherence and NAcc activity during the motor target and outcome phases of the task, and also for incentive loss conditions (see Supplementary Fig. 5). Similar to anticipatory activity, AIns-NAcc tract coherence was associated with decreased NAcc activity when participants responded to targets for non-gains (right: β=-0.30, t(89)=-2.95, p < 0.01; left: β=-0.39, t(89)=-4.03, p < 0.001).

Whereas animal axon-tracings indicate that the AIns projects unidirectionally to the NAcc, in the current study AIns-NAcc tract coherence was also associated with greater AIns activity during the anticipation of losses (right: β = 0.27, $t(89) = 2.72$, $p < 0.01$; left: β=0.31, $t(89) = 3.06$, $p < 0.01$), but with lesser AIns activity during the anticipation of non-gains (right: β=-0.20, $t(89)$=-1.96, $p = 0.05$; left: β=-0.32, $t(89)$=-3.24, $p < 0.01$). The tract was not associated with AIns activity in anticipation of non-losses (right: β=-0.01, t(89)=-0.13, p=0.89; left: β=0.05, t(89)=0.44, p=0.66) and gains (right: β=0.05, t(89)=0.46, p=0.65; left: β=-0.06, t(89)=-0.54, p=0.59).

3.4. Structural tract coherence of AIns-NAcc and NAcc activity predicts future SPSRQ-C drive

AIns-NAcc tract coherence predicted greater SPSRQ-C drive reported two years later (β = 0.28, $t(67) = 2.41$, $p = 0.02$). This association remained statistically significant after controlling for sex, age, and SPSRQ-C drive at baseline (AIns-NAcc tract coherence: β=0.20, $t(64) = 2.01$, $p < 0.05$; female: β=-0.22, $t(64)$=-2.00, $p < 0.05$; age: β=0.09, $t(64) = 0.79$, $p = 0.43$; baseline SPSRQ-C drive: β=0.41, $t(64) = 3.93$, $p < 0.001$). AIns-NAcc tract coherence was not associated with baseline SPSRQ-C drive (β=0.12, $t(67) = 0.99$, $p = 0.32$) or with either baseline or follow-up SPSRQ-C impulsivity (baseline: β=0.08, $t(67) = 0.67$, $p = 0.51$; follow-up: β=0.08, $t(67) = 0.64$, $p = 0.52$). Finally, AIns-NAcc tract coherence was not associated with scores on any other subscale on the SPSRQ-C (see Supplementary Table 1).

We then tested whether individual differences in NAcc functional activity could statistically mediate the direct path from AIns-NAcc tract coherence to future SPSRQ-C drive (see Fig. 5). Bootstrapped path analysis (samples = 10,000), which included the same covariates of no interest as were included in the pairwise regressions, indicated that greater AIns-NAcc tract coherence was associated with reduced NAcc activity during non-gain anticipation (a: β=-0.36, $p < 0.01$), and that reduced NAcc activity for non-gains was associated with increased future SPSRQ-C drive (b: β=-0.19, $p = 0.04$). Including the indirect effect of NAcc activity for non-gains reduced the direct association of AIns-

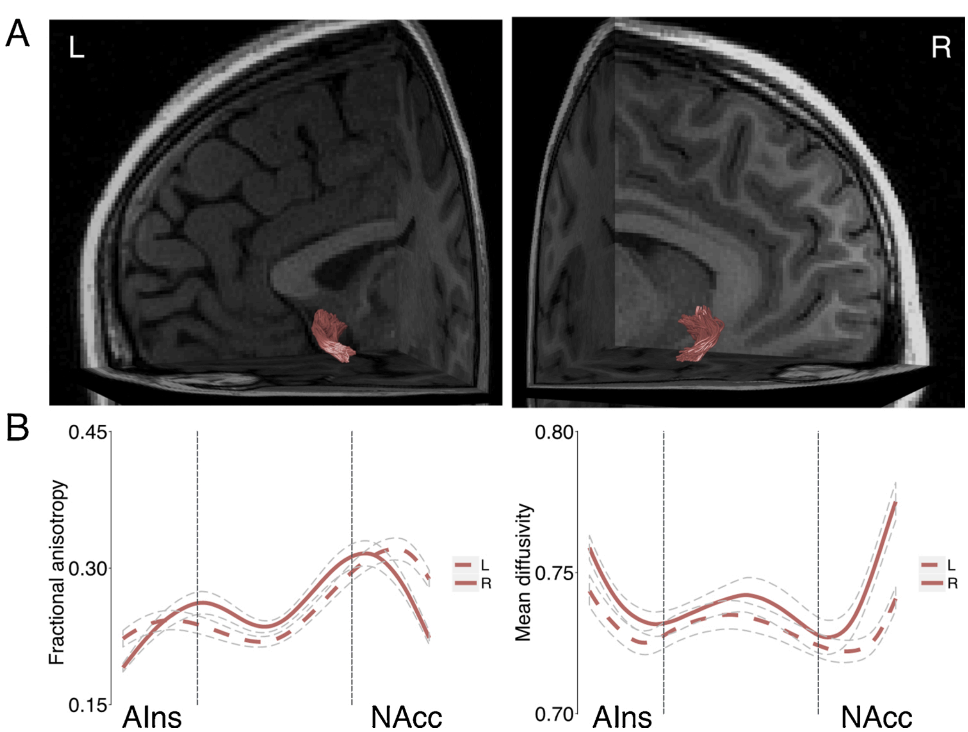

Fig. 3. Visualization of the anterior insula to nucleus accumbens tract.
(A) The AIns-NAcc tract in both hemispheres in a representative participant. The AIns-NAcc tract begins in the anterior insula and travels along the lateral-medial axis within subcaudate white matter until terminating in the NAcc (Leong et al., 2016, 2018). See Supplementary Fig. 3 for tract visualizations in additional participants. See also Supplementary Fig. 4 for the fiber orientation distribution in the voxels through which the AIns-NAcc tract travels.
(B) Tract profiles of AIns-NAcc tract fractional anisotropy (FA) along the trajectory of the tract. Mean diffusivity is also plotted to demonstrate the inverse relation between mean diffusivity and FA. The FA values in the middle 50% of the tract were averaged in each hemisphere separately to derive a measure of tract coherence in every participant.

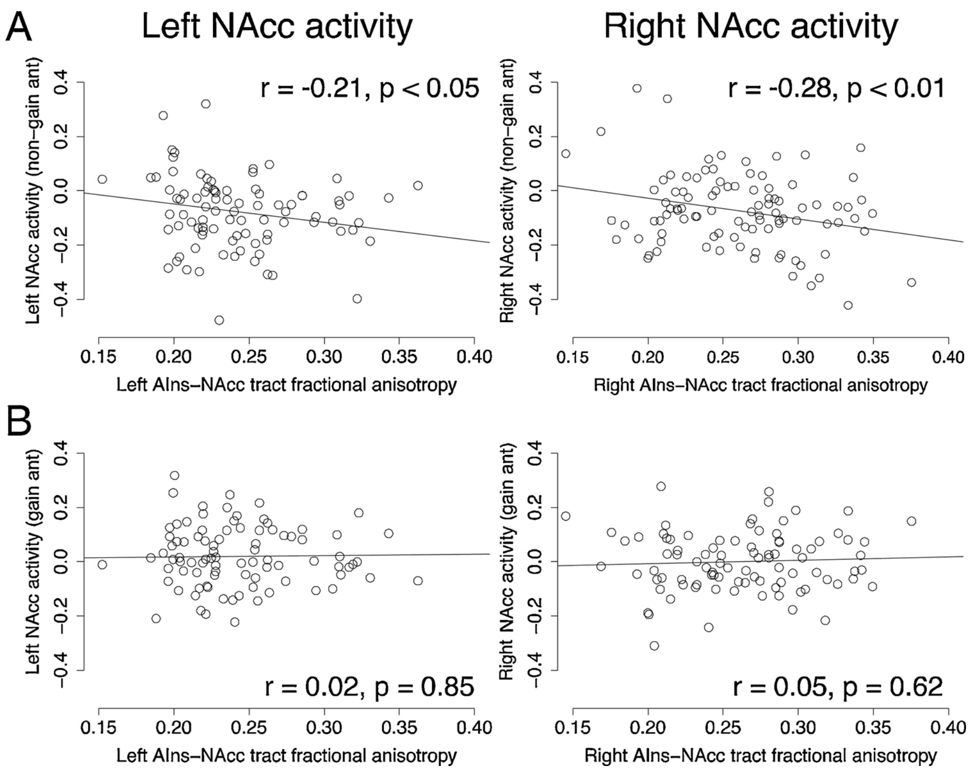

Fig. 4. Structural coherence of the AIns-NAcc tract is associated with diminished NAcc activity during anticipation of non-gains.
(A) The effect of AIns-NAcc tract coherence (mean fractional anisotropy) on NAcc activity is driven by decreased NAcc activity when participants anticipated non-gains (right: β=-0.28, $t(89)$=-2.70, $p < 0.01$; left: β=-0.21, $t(89)$=-2.02, $p < 0.05$). Bootstrapped correlations could demonstrate the robustness of the association in the right hemisphere (samples=10,000; right: $p = 0.02$; left: $p = 0.09$). A non-parametric Spearman's correlation could confirm the robustness of the association in both hemispheres (rho: -0.20, 95 % confidence interval: -0.39, -0.003).
(B) AIns-NAcc tract coherence (mean fractional anisotropy) was not associated with NAcc activity when participants anticipated gains (right: β = 0.05, $t(89) = 0.50$, $p = 0.62$; left: β=0.02, $t(89) = 0.19$, $p = 0.85$). All regression coefficients are standardized. See Supplementary Fig. 5 for associations between AIns-NAcc tract coherence and functional activity from other trial phases.

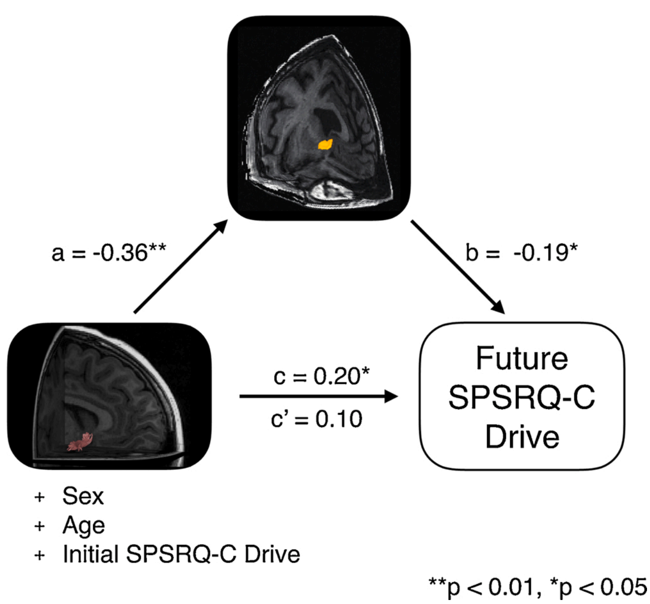

Fig. 5. NAcc activity to non-gains statistically mediates the association between AIns-NAcc structural coherence and SPSRQ-C drive at follow-up.
Statistical mediation analysis of a model in which AIns-NAcc tract coherence correlates with greater future SPSRQ-C drive through decreased NAcc activity during non-gain anticipation. The model includes sex, age, and initial SPSRQ-C drive as covariates of no interest. AIns-NAcc tract coherence was associated with greater future SPSRQ-C drive (c). The indirect pathway statistically mediated this association, such that AIns-NAcc tract coherence was associated with decreased NAcc activity (a), and NAcc activity was associated with decreased future drive (b). Including functional NAcc activity as a mediating variable reduced the direct pathway to no statistical significance (c').

NAcc tract coherence with future SPSRQ-C drive to non-significance (c': β=0.10, $p = 0.36$). The results from the mediation analysis based on the prespecified spherical NAcc VOI were similar when activity was extracted from a probabilistic atlas NAcc VOI (a: β=-0.37, $p < 0.01$; b: β=-0.23, $p = 0.01$; c': β=0.09, $p = 0.45$).

4. Discussion

In this study, we characterized the white-matter tract connecting the AIns to the NAcc for the first time in adolescent humans. We found that structural coherence of the AIns-NAcc tract, indexed by FA, was associated with decreased NAcc activity during anticipation of non-gain incentives in a monetary incentive delay task. Structural coherence of the AIns-NAcc tract prospectively predicted greater motivation two years later, assessed by participants' scores on the SPSRQ-C. Anticipatory NAcc activity could statistically mediate the association between anatomical structure and motivation reported two years later. Together, our findings demonstrate the utility of using multimodal neuroimaging to characterize targeted white-matter tracts in linking brain structure to brain function to future motivated behavior.

This study extends the previous finding in adults that greater coherence of the AIns-NAcc tract is associated with reduced NAcc activity prior to engaging in a risky choice, which in turn is linked to reduced preference for positively skewed gambles (Leong et al., 2016). The present findings suggest that this structural connection also influences anticipatory reward responses in adolescents. Adolescence is a developmental period during which potential rewards in the environment elicit stronger responses in the mesolimbic brain regions innervated by dopamine (Somerville et al., 2010). Greater mesolimbic brain activity can facilitate increased exploration of novel environments and experiences, which may help adolescents achieve independence as they move toward adulthood (Spear, 2011; Galván, 2013; Walker et al., 2017). Comparative research provides converging evidence that adolescent rats learn less from negative feedback than their younger and older counterparts (Pattwell et al., 2011, 2012; Pattwell et al., 2016,). Consistent with these findings, studies with humans suggest that adolescents have less brain activation in response to potential losses and aversive outcomes than do adults (Doremus-Fitzwater and Spear, 2016; Insel and Somerville, 2018). Tasks administered to adolescent humans that pit potential gains versus losses within a single choice, as in risky gambling, and that separate reward anticipation versus reward receipt, may help to elucidate the influence of the AIns-NAcc tract on anticipatory NAcc activity (Wu et al., 2011; Leong et al., 2016).

The present study does not yet fit intuitively in the existing landscape of adolescent brain research. The current findings suggest that AIns-NAcc tract coherence is associated with reduced NAcc activity during anticipation of non-gain incentives in adolescents. However, AIns-NAcc tract coherence was also associated with greater NAcc activity during anticipation of losses (see Supplementary Fig. 5). In reconciling these findings with the broader literature, we posit that AIns to NAcc projections do not yet fully modulate the NAcc's responses to potential gains and losses in early adolescence. Whereas the coherence of white matter near the AIns-NAcc tract (i.e., in the uncinate fasciculus) increases from adolescence to adulthood (Lebel et al., 2008; Simmonds et al., 2014), NAcc activity in response to reward outcomes peaks at age 15 and decreases with age (Braams et al., 2015; Schreuders et al., 2018; Insel and Somerville, 2018). Thus, our finding may reflect a period in early adolescence during which AIns-NAcc tract is modulating NAcc activity in different reward contexts. Longitudinal studies can identify more precisely whether AIns-NAcc tract coherence increases during adolescence, and then link increases in tract coherence to reduced NAcc activity during anticipation of rewards. Future studies should also separately target NAcc activity in response to reward outcomes. Finally, modeling approaches such as dynamic causal modeling might be used to test whether the AIns-NAcc tract moderates the effect of AIns activity on NAcc activity (Cho et al., 2013).

The present findings provides specific hypotheses to test in large multimodal neuroimaging datasets. For example, in the Adolescent Brain Cognitive Development (ABCD) study, longitudinal data are obtained from both FMRI during a monetary incentive delay task and diffusion MRI in over 11,000 adolescents (Casey et al., 2018). The ABCD dataset also includes behavioral and self-report indices of approach, avoidance, and impulse control, as well as potential moderating variables (e.g., ethnicity, socioeconomic status), that researchers can use to examine links between brain and behavior (Luciana et al., 2018). Thus, findings from the present study might be replicated and extended by linking the structure and function of the AIns-NAcc pathway to relevant constructs assessed at baseline and at future time points. These brain measures may additionally precede and predict future real-life outcomes, including drug abuse and psychiatric disorders (Büchel et al., 2017).

Future research might also integrate the present findings with morphological changes in the NAcc during adolescence. Previous studies have indicated that NAcc volume decreases linearly from childhood to adulthood (Mills et al., 2014; Mills et al., 2016; Herting et al., 2018; Wierenga et al., 2018), which suggests that morphologically changes in the NAcc might drive increased reward sensitivity and motivated behaviors in adolescents. However, no research has explored links between anatomical projections to the NAcc and NAcc morphology. Establishing links between structural tracts, functional activity, and morphology will clarify the concerted unfolding of adolescent brain development.

We should note three limitations of this study. First, the adaptive algorithm to control participants' hit rate in the KIDMID task was set to 66 % across all conditions rather than within each condition as in the original MID task (Knutson et al., 2001). This task design led to different behavioral performance and reaction times across conditions, such that participants responded more quickly to incentivized than to non-incentivized trials (see Fig. 1). One important advantage of the task design, however, is that it allowed us to compare reaction times across task conditions; indeed, our analyses replicated previous findings that increased self-report drive and impulsivity are correlated with faster reaction times to achieve gains and avoid losses (Colder et al., 2011; see Supplementary Fig. 1). Second, we focused on a narrow window of development (i.e., early adolescence ages 9–13 years), and studied an imbalanced sample that included more female than male participants. Future studies should track brain development longitudinally across a longer time span, and recruit a comparable number of female and male participants, which will allow researchers to characterize the development of the AIns-NAcc circuit with greater generalizability and to explore possible sex differences. Finally, diffusion tensor metrics such as FA can only provide a crude estimate of the structural coherence of a tract, and the tracts that cross the AIns-NAcc tract further decrease the validity of the measure (Jones et al., 2013). Novel diffusion MRI techniques such as Neurite Orientation Dispersion and Density Imaging (NODDI) might eventually support or supplant the more traditional measures used in this study (Zhang et al., 2012). Future comparative research that pairs diffusion MRI with physiological manipulations such as CLARITY might help validate specific neuroimaging measures as well (Leuze et al., 2017).

While this study could characterize the structure and function of the AIns-NAcc circuit, many converging circuits contribute together to motivated behavior. Further research should specifically examine the circuits that guide incentivized impulses, including dopaminergic projections from the ventral tegmental area to the NAcc (MacNiven et al., 2020), glutamatergic connections from the medial PFC and amygdala to NAcc (Samanez-Larkin et al., 2012; Leong et al., 2016; Hampton et al., 2017; Jung et al., 2018), and reciprocal connections between the AIns and ventrolateral PFC (Leong et al., 2018). Distinct connections to the NAcc may support dissociable aspects of motivated behavior. Advancing models that link brain structure, function, and behavior in human adolescence might then inform policy and pedagogy targeted at this life stage.

Author contributions

I.H.G., J.K.L., N.L.C., and T.C.H. designed the research. L.S. and N.L. C acquired the data. J.K.L., L.S., and T.C.H. analyzed the data. All authors wrote the paper.

Declaration of Competing Interest

The authors declare that they have no known competing financial interests or personal relationships that could have appeared to influence the work reported in this paper.

Acknowledgments

This work was supported by the National Institute of Mental Health (R37MH101495 to IHG, T32MH020006 to JKL, F32MH114317 to NLC, K01MH117442 to TCH), the Klingenstein Third Generation Foundation (Fellowship Award in Child and Adolescent Depression to TCH), the National Science Foundation (Graduate Student Research Fellowship to NLC), the Stanford University Precision Health and Integrated Diagnostics (IHG and TCH), and a Neuroscience Institute Stanford NeuroChoice Initiative grant to BK. The funding agencies played no role in the design and conduct of the study; collection, management, analysis, and interpretation of the data; and preparation, review, or approval of the manuscript. We wish to thank Cat Camacho, Monica Ellwood-Lowe, Meghan Goyer, Kira Oskirko, Holly Pham, Morgan Popolizio, Alexandra Price, and Sophie Schouboe for assistance with data collection and organization. Finally, we wish to thank the participants and their families for contributing to the study.

Appendix A. Supplementary data

Supplementary material related to this article can be found, in the online version, at doi:https://doi.org/10.1016/j.dcn.2020.100881.

References

Braams, B.R., van Duijvenvoorde, A.C.K., Peper, J.S., Crone, E.A., 2015. Longitudinal changes in adolescent risk-taking: a comprehensive study of neural responses to rewards, pubertal development, and risk-taking behavior. J. Neurosci. 35 (18), 7226–7238. https://doi.org/10.1523/JNEUROSCI.4764-14.2015.

Büchel, C., Peters, J., Banaschewski, T., Bokde, A.L.W., Bromberg, U., Conrod, P.J., Flor, H., Papadopoulos, D., Garavan, H., Gowland, P., Heinz, A., Walter, H., Ittermann, B., Mann, K., Martinot, J.-L., Paillère-Martinot, M.-L., Nees, F., Paus, T., Pausova, Z., et al., 2017. Blunted ventral striatal responses to anticipated rewards foreshadow problematic drug use in novelty-seeking adolescents. Nat. Commun. 8, 14140. https://doi.org/10.1038/ncomms14140.

Casey, B.J., Cannonier, T., Conley, M.I., Cohen, A.O., Barch, D.M., Heitzeg, M.M., Soules, M.E., Teslovich, T., Dellarco, D.V., Garavan, H., Orr, C.A., Wager, T.D., Banich, M.T., Speer, N.K., Sutherland, M.T., Riedel, M.C., Dick, A.S., Bjork, J.M., Thomas, K.M., et al., 2018. The adolescent brain cognitive development (ABCD) study: imaging acquisition across 21 sites. Dev. Cogn. Neurosci. 32, 43–54. https://doi.org/10.1016/j.dcn.2018.03.001.

Chikama, M., McFarland, N.R., Amaral, D.G., Haber, S.N., 1997. Insular cortical projections to functional regions of the striatum correlate with cortical cytoarchitectonic organization in the primate. J. Neurosci. 17 (24), 9686–9705. https://www.ncbi.nlm.nih.gov/pubmed/9391023.

Cho, Y.T., Fromm, S., Guyer, A.E., Detloff, A., Pine, D.S., Fudge, J.L., Ernst, M., 2013. Nucleus accumbens, thalamus and insula connectivity during incentive anticipation in typical adults and adolescents. NeuroImage 66, 508–521. https://doi.org/10.1016/j.neuroimage.2012.10.013.

Clark, L., Studer, B., Bruss, J., Tranel, D., Bechara, A., 2014. Damage to insula abolishes cognitive distortions during simulated gambling. Proc. Natl. Acad. Sci. U. S. A. 111 (16), 6098–6103. https://doi.org/10.1073/pnas.1322295111.

Cohen, M.S., 1997. Parametric analysis of fMRI data using linear systems methods. NeuroImage 6 (2), 93–103. https://doi.org/10.1006/nimg.1997.0278.

Colder, C.R., O'Connor, R.M., 2004. Gray's reinforcement sensitivity model and child psychopathology: laboratory and questionnaire assessment of the BAS and BIS. J. Abnorm. Child Psychol. 32 (4), 435–451. https://doi.org/10.1023/b:jacp.0000030296.54122.b6.

Colder, C.R., Trucco, E.M., Lopez, H.I., Hawk Jr., L.W., Read, J.P., Lengua, L.J., Weiczorek, W.F., Eiden, R.D., 2011. Revised reinforcement sensitivity theory and laboratory assessment of BIS and BAS in children. J. Res. Pers. 45 (2), 198–207. https://doi.org/10.1016/j.jrp.2011.01.005.

Coleman, L., Coleman, J., 2002. The measurement of puberty: a review. J. Adolesc. 25 (5), 535–550. https://doi.org/10.1006/jado.2002.0494.

Colich, N.L., Williams, E.S., Ho, T.C., King, L.S., Humphreys, K.L., Price, A.N., Ordaz, S. J., Gotlib, I.H., 2017. The association between early life stress and prefrontal cortex activation during implicit emotion regulation is moderated by sex in early adolescence. Dev. Psychopathol. 29 (5), 1851–1864. https://doi.org/10.1017/S0954579417001444.

Cox, R.W., 1996. AFNI: software for analysis and visualization of functional magnetic resonance neuroimages. Comput. Biomed. Res. 29 (3), 162–173. https://doi.org/10.1006/cbmr.1996.0014.

Cox, R.W., Chen, G., Glen, D.R., Reynolds, R.C., Taylor, P.A., 2017. fMRI clustering and false-positive rates [Review of *fMRI clustering and false-positive rates*]. Proc. Natl. Acad. Sci. U. S. A. 114 (17), E3370–E3371. https://doi.org/10.1073/pnas.1614961114.

Craig, A.D.B., 2009. How do you feel–now? The anterior insula and human awareness. Nat. Rev. Neurosci. 10 (1), 59–70. https://doi.org/10.1038/nrn2555.

Dahl, R.E., Allen, N.B., Wilbrecht, L., Suleiman, A.B., 2018. Importance of investing in adolescence from a developmental science perspective. Nature 554 (7693), 441–450. https://doi.org/10.1038/nature25770.

Davidow, J.Y., Foerde, K., Galván, A., Shohamy, D., 2016. An upside to reward sensitivity: the hippocampus supports enhanced reinforcement learning in adolescence. Neuron 92 (1), 93–99. https://doi.org/10.1016/j.neuron.2016.08.031.

Desikan, R.S., Ségonne, F., Fischl, B., Quinn, B.T., Dickerson, B.C., Blacker, D., Buckner, R.L., Dale, A.M., Maguire, R.P., Hyman, B.T., Albert, M.S., Killiany, R.J., 2006. An automated labeling system for subdividing the human cerebral cortex on MRI scans into gyral based regions of interest. NeuroImage 31 (3), 968–980. https://doi.org/10.1016/j.neuroimage.2006.01.021.

Destrieux, C., Fischl, B., Dale, A., Halgren, E., 2010. Automatic parcellation of human cortical gyri and sulci using standard anatomical nomenclature. NeuroImage 53 (1), 1–15. https://doi.org/10.1016/j.neuroimage.2010.06.010.

Doremus-Fitzwater, T.L., Spear, L.P., 2016. Reward-centricity and attenuated aversions: an adolescent phenotype emerging from studies in laboratory animals. Neurosci. Biobehav. Rev. 70, 121–134. https://doi.org/10.1016/j.neubiorev.2016.08.015.

Eaton, D.K., Kann, L., Kinchen, S., Shanklin, S., Flint, K.H., Hawkins, J., Harris, W.A., Lowry, R., McManus, T., Chyen, D., Others, 2012. Youth risk behavior surveillance—United States, 2011. In: Morbidity Mortality Weekly Report. Surveillance Summaries: MMWR / Centers for Disease Control, 61, pp. 1–162 (4).

Ferenczi, E.A., Zalocusky, K.A., Liston, C., Grosenick, L., Warden, M.R., Amatya, D., Katovich, K., Mehta, H., Patenaude, B., Ramakrishnan, C., Kalanithi, P., Etkin, A., Knutson, B., Glover, G.H., Deisseroth, K., 2016. Prefrontal cortical regulation of brainwide circuit dynamics and reward-related behavior. Science 351 (6268), aac9698. https://doi.org/10.1126/science.aac9698.

Fischl, B., 2012. FreeSurfer. NeuroImage 62 (2), 774–781. https://doi.org/10.1016/j.neuroimage.2012.01.021.

Fischl, B., van der Kouwe, A., Destrieux, C., Halgren, E., Ségonne, F., Salat, D.H., Busa, E., Seidman, L.J., Goldstein, J., Kennedy, D., Caviness, V., Makris, N., Rosen, B., Dale, A. M., 2004. Automatically parcellating the human cerebral cortex. Cereb. Cortex 14 (1), 11–22. https://doi.org/10.1093/cercor/bhg087.

Foulkes, L., Blakemore, S.-J., 2018. Studying individual differences in human adolescent brain development. Nat. Neurosci. 21 (3), 315–323. https://doi.org/10.1038/s41593-018-0078-4.

Galván, A., 2013. The teenage brain: sensitivity to rewards. Curr. Dir. Psychol. Sci. https://doi.org/10.1177/0963721413480859.

Gotlib, I.H., Hamilton, J.P., Cooney, R.E., Singh, M.K., Henry, M.L., Joormann, J., 2010. Neural processing of reward and loss in girls at risk for major depression. Arch. Gen. Psychiatry 67 (4), 380–387. https://doi.org/10.1001/archgenpsychiatry.2010.13.

Haber, S.N., Knutson, B., 2010. The reward circuit: linking primate anatomy and human imaging. Neuropsychopharmacology 35 (1), 4–26. https://doi.org/10.1038/npp.2009.129.

Hampton, W.H., Alm, K.H., Venkatraman, V., Nugiel, T., Olson, I.R., 2017. Dissociable frontostriatal white matter connectivity underlies reward and motor impulsivity. NeuroImage 150, 336–343. https://doi.org/10.1016/j.neuroimage.2017.02.021.

Herting, M.M., Maxwell, E.C., Irvine, C., Nagel, B.J., 2012. The impact of sex, puberty, and hormones on white matter microstructure in adolescents. Cereb. Cortex 22 (9), 1979–1992. https://doi.org/10.1093/cercor/bhr246.

Herting, M.M., Johnson, C., Mills, K.L., Vijayakumar, N., Dennison, M., Liu, C., Goddings, A.-L., Dahl, R.E., Sowell, E.R., Whittle, S., Allen, N.B., Tamnes, C.K., 2018. Development of subcortical volumes across adolescence in males and females: a multisample study of longitudinal changes. NeuroImage 172, 194–205. https://doi.org/10.1016/j.neuroimage.2018.01.020.

Ho, T.C., King, L.S., Leong, J.K., Colich, N.L., Humphreys, K.L., Ordaz, S.J., Gotlib, I.H., 2017. Effects of sensitivity to life stress on uncinate fasciculus segments in early adolescence. Soc. Cogn. Affect. Neurosci. 12 (9), 1460–1469. https://doi.org/10.1093/scan/nsx065.

Ikemoto, S., Panksepp, J., 1999. The role of nucleus accumbens dopamine in motivated behavior: a unifying interpretation with special reference to reward-seeking. Brain Res. Rev. 31 (1), 6–41. https://doi.org/10.1016/s0165-0173(99)00023-5.

Insel, C., Somerville, L.H., 2018. Asymmetric neural tracking of gain and loss magnitude during adolescence. Soc. Cogn. Affect. Neurosci. 13 (8), 785–796. https://doi.org/10.1093/scan/nsy058.

Jones, D.K., Knösche, T.R., Turner, R., 2013. White matter integrity, fiber count, and other fallacies: the doös and don'ts of diffusion MRI. NeuroImage 73, 239–254. https://doi.org/10.1016/j.neuroimage.2012.06.081.

Jung, W.H., Lee, S., Lerman, C., Kable, J.W., 2018. Amygdala functional and structural connectivity predicts individual risk tolerance. Neuron 98 (2), 394–404. https://doi.org/10.1016/j.neuron.2018.03.019 e4.

King, L.S., Colich, N.L., LeMoult, J., Humphreys, K.L., Ordaz, S.J., Price, A.N., Gotlib, I. H., 2017. The impact of the severity of early life stress on diurnal cortisol: the role of puberty. Psychoneuroendocrinology 77, 68–74. https://doi.org/10.1016/j.psyneuen.2016.11.024.

Knutson, B., Adams, C.M., Fong, G.W., Hommer, D., 2001. Anticipation of increasing monetary reward selectively recruits nucleus accumbens. J. Neurosci. 21 (16), RC159. https://doi.org/10.1523/JNEUROSCI.21-16-j0002.2001.

Knutson, B., Bossaerts, P., 2007. Neural antecedents of financial decisions. J. Neurosci. 27 (31), 8174–8177. https://doi.org/10.1523/JNEUROSCI.1564-07.2007.

Knutson, B., Greer, S.M., 2008. Anticipatory affect: neural correlates and consequences for choice. Philos. Trans. R. Soc. Lond., B, Biol. Sci. 363 (1511), 3771–3786. https://doi.org/10.1098/rstb.2008.0155.

Knutson, B., Katovich, K., Suri, G., 2014. Inferring affect from fMRI data. Trends Cogn. Sci. 18 (8), 422–428. https://doi.org/10.1016/j.tics.2014.04.006.

Kuhnen, C.M., Knutson, B., 2005. The neural basis of financial risk taking. Neuron 47 (5), 763–770. https://doi.org/10.1016/j.neuron.2005.08.008.

Lebel, C., Walker, L., Leemans, A., Phillips, L., Beaulieu, C., 2008. Microstructural maturation of the human brain from childhood to adulthood. NeuroImage 40 (3), 1044–1055. https://doi.org/10.1016/j.neuroimage.2007.12.053.

Leong, J.K., Pestilli, F., Wu, C.C., Samanez-Larkin, G.R., Knutson, B., 2016. White-matter tract connecting anterior insula to nucleus accumbens correlates with reduced preference for positively skewed gambles. Neuron 89 (1), 63–69. https://doi.org/10.1016/j.neuron.2015.12.015.

Leong, J.K., MacNiven, K.H., Samanez-Larkin, G.R., Knutson, B., 2018. Distinct neural circuits support incentivized inhibition. NeuroImage 178, 435–444. https://doi.org/10.1016/j.neuroimage.2018.05.055.

Leuze, C., Aswendt, M., Ferenczi, E., Liu, C.W., Hsueh, B., Goubran, M., Tian, Q., Steinberg, G., Zeineh, M.M., Deisseroth, K., McNab, J.A., 2017. The separate effects of lipids and proteins on brain MRI contrast revealed through tissue clearing. NeuroImage 156, 412–422. https://doi.org/10.1016/j.neuroimage.2017.04.021.

Luciana, M., Bjork, J.M., Nagel, B.J., Barch, D.M., Gonzalez, R., Nixon, S.J., Banich, M.T., 2018. Adolescent neurocognitive development and impacts of substance use: overview of the adolescent brain cognitive development (ABCD) baseline neurocognition battery. Dev. Cogn. Neurosci. 32, 67–79. https://doi.org/10.1016/j.dcn.2018.02.006.

MacNiven, K.H., Leong, J.K., Knutson, B., 2020. Medial forebrain bundle structure is linked to human impulsivity. Sci. Adv. 6 (38), eaba4788. https://doi.org/10.1126/sciadv.aba4788.

Marshall, W.A., Tanner, J.M., 1969. Variations in pattern of pubertal changes in girls. Arch. Dis. Child. 44 (235), 291–303. https://doi.org/10.1136/adc.44.235.291.

Mills, K.L., Goddings, A.-L., Clasen, L.S., Giedd, J.N., Blakemore, S.-J., 2014. The developmental mismatch in structural brain maturation during adolescence. Dev. Neurosci. 36 (3-4), 147–160. https://doi.org/10.1159/000362328.

Mills, K.L., Goddings, A.-L., Herting, M.M., Meuwese, R., Blakemore, S.-J., Crone, E.A., Dahl, R.E., Güroğlu, B., Raznahan, A., Sowell, E.R., Tamnes, C.K., 2016. Structural brain development between childhood and adulthood: Convergence across four

longitudinal samples. NeuroImage 141, 273–281. https://doi.org/10.1016/j.neuroimage.2016.07.044.
Morris, N.M., Udry, J.R., 1980. Validation of a self-administered instrument to assess stage of adolescent development. J. Youth Adolesc. 9 (3), 271–280. https://doi.org/10.1007/BF02088471.
Palminteri, S., Justo, D., Jauffret, C., Pavlicek, B., Dauta, A., Delmaire, C., Czernecki, V., Karachi, C., Capelle, L., Durr, A., Pessiglione, M., 2012. Critical roles for anterior insula and dorsal striatum in punishment-based avoidance learning. Neuron 76 (5), 998–1009. https://doi.org/10.1016/j.neuron.2012.10.017.
Pattwell, S.S., Bath, K.G., Casey, B.J., Ninan, I., Lee, F.S., 2011. Selective early-acquired fear memories undergo temporary suppression during adolescence. Proc. Natl. Acad. Sci. U. S. A. 108 (3), 1182–1187. https://doi.org/10.1073/pnas.1012975108.
Pattwell, S.S., Duhoux, S., Hartley, C.A., Johnson, D.C., Jing, D., Elliott, M.D., Ruberry, E. J., Powers, A., Mehta, N., Yang, R.R., Soliman, F., Glatt, C.E., Casey, B.J., Ninan, I., Lee, F.S., 2012. Altered fear learning across development in both mouse and human. Proc. Natl. Acad. Sci. U. S. A. 109 (40), 16318–16323. https://doi.org/10.1073/pnas.1206834109.
Pattwell, S.S., Liston, C., Jing, D., Ninan, I., Yang, R.R., Witztum, J., Murdock, M.H., Dincheva, I., Bath, K.G., Casey, B.J., Deisseroth, K., Lee, F.S., 2016. Dynamic changes in neural circuitry during adolescence are associated with persistent attenuation of fear memories. Nat. Commun. 7, 11475. https://doi.org/10.1038/ncomms11475.
Reynolds, S.M., Zahm, D.S., 2005. Specificity in the projections of prefrontal and insular cortex to ventral striatopallidum and the extended amygdala. J. Neurosci. 25 (50), 11757–11767. https://doi.org/10.1523/JNEUROSCI.3432-05.2005.
Samanez-Larkin, G.R., Knutson, B., 2015. Decision making in the ageing brain: changes in affective and motivational circuits. Nat. Rev. Neurosci. 16 (5), 278–289. https://doi.org/10.1038/nrn3917.
Samanez-Larkin, G.R., Levens, S.M., Perry, L.M., Dougherty, R.F., Knutson, B., 2012. Frontostriatal white matter integrity mediates adult age differences in probabilistic reward learning. J. Neurosci. 32 (15), 5333–5337. https://doi.org/10.1523/JNEUROSCI.5756-11.2012.
Schreuders, E., Braams, B.R., Blankenstein, N.E., Peper, J.S., Güroğlu, B., Crone, E.A., 2018. Contributions of reward sensitivity to ventral striatum activity across adolescence and early adulthood. Child Dev. 89 (3), 797–810. https://doi.org/10.1111/cdev.13056.
Shirtcliff, E.A., Dahl, R.E., Pollak, S.D., 2009. Pubertal development: correspondence between hormonal and physical development. Child Dev. 80 (2), 327–337. https://doi.org/10.1111/j.1467-8624.2009.01263.x.
Simmonds, D.J., Hallquist, M.N., Asato, M., Luna, B., 2014. Developmental stages and sex differences of white matter and behavioral development through adolescence: a longitudinal diffusion tensor imaging (DTI) study. NeuroImage 92, 356–368. https://doi.org/10.1016/j.neuroimage.2013.12.044.
Sisk, C.L., Foster, D.L., 2004. The neural basis of puberty and adolescence. Nat. Neurosci. 7 (10), 1040–1047. https://doi.org/10.1038/nn1326.
Somerville, L.H., Jones, R.M., Casey, B.J., 2010. A time of change: behavioral and neural correlates of adolescent sensitivity to appetitive and aversive environmental cues. Brain Cogn. 72 (1), 124–133. https://doi.org/10.1016/j.bandc.2009.07.003.
Spear, L.P., 2000. The adolescent brain and age-related behavioral manifestations. Neurosci. Biobehav. Rev. 24 (4), 417–463. https://doi.org/10.1016/s0149-7634(00)00014-2.
Spear, L.P., 2011. Rewards, aversions and affect in adolescence: emerging convergences across laboratory animal and human data. Dev. Cogn. Neurosci. 1 (4), 392–400. https://doi.org/10.1016/j.dcn.2011.08.001.
Steinberg, L., Graham, S., O'Brien, L., Woolard, J., Cauffman, E., Banich, M., 2009. Age differences in future orientation and delay discounting. Child Dev. 80 (1), 28–44. https://doi.org/10.1111/j.1467-8624.2008.01244.x.
Substance Abuse and Mental Health Services Administration (SAMHSA), 2012. National Survey on Drug Use and Health (NSDUH). S. Prepared by Office of Applied Studies (OAS), and by RTI International (RTI International Is a Trade Name of Research Triangle Institute). Substance Abuse and Mental Health Services Administration, Rockville, MD.
Telzer, E.H., 2016. Dopaminergic reward sensitivity can promote adolescent health: a new perspective on the mechanism of ventral striatum activation. Dev. Cogn. Neurosci. 17, 57–67. https://doi.org/10.1016/j.dcn.2015.10.010.
Torrubia, R., Ávila, C., Moltó, J., Caseras, X., 2001. The Sensitivity to Punishment and Sensitivity to reward Questionnaire (SPSRQ) as a measure of Gray's anxiety and impulsivity dimensions. Pers. Individ. Dif. 31 (6), 837–862. https://doi.org/10.1016/S0191-8869(00)00183-5.
Tournier, J.-D., Calamante, F., Connelly, A., 2007. Robust determination of the fibre orientation distribution in diffusion MRI: non-negativity constrained super-resolved spherical deconvolution. NeuroImage 35 (4), 1459–1472. https://doi.org/10.1016/j.neuroimage.2007.02.016.
Walker, D.M., Bell, M.R., Flores, C., Gulley, J.M., Willing, J., Paul, M.J., 2017. Adolescence and reward: making sense of neural and behavioral changes amid the Chaos. J. Neurosci. 37 (45), 10855–10866. https://doi.org/10.1523/JNEUROSCI.1834-17.2017.
Wierenga, L.M., Bos, M.G.N., Schreuders, E., Vd Kamp, F., Peper, J.S., Tamnes, C.K., Crone, E.A., 2018. Unraveling age, puberty and testosterone effects on subcortical brain development across adolescence. Psychoneuroendocrinology 91, 105–114. https://doi.org/10.1016/j.psyneuen.2018.02.034.
Wu, C.C., Bossaerts, P., Knutson, B., 2011. The affective impact of financial skewness on neural activity and choice. PLoS One 6 (2), e16838. https://doi.org/10.1371/journal.pone.0016838.
Yeatman, J.D., Dougherty, R.F., Myall, N.J., Wandell, B.A., Feldman, H.M., 2012. Tract profiles of white matter properties: automating fiber-tract quantification. PLoS One 7 (11), e49790. https://doi.org/10.1371/journal.pone.0049790.
Zhang, H., Schneider, T., Wheeler-Kingshott, C.A., Alexander, D.C., 2012. NODDI: practical in vivo neurite orientation dispersion and density imaging of the human brain. NeuroImage 61 (4), 1000–1016. https://doi.org/10.1016/j.neuroimage.2012.03.072.

Supplementary Figure 1. SPSRQ-C drive and impulsivity are correlated with faster reaction times in the KIDMID task.

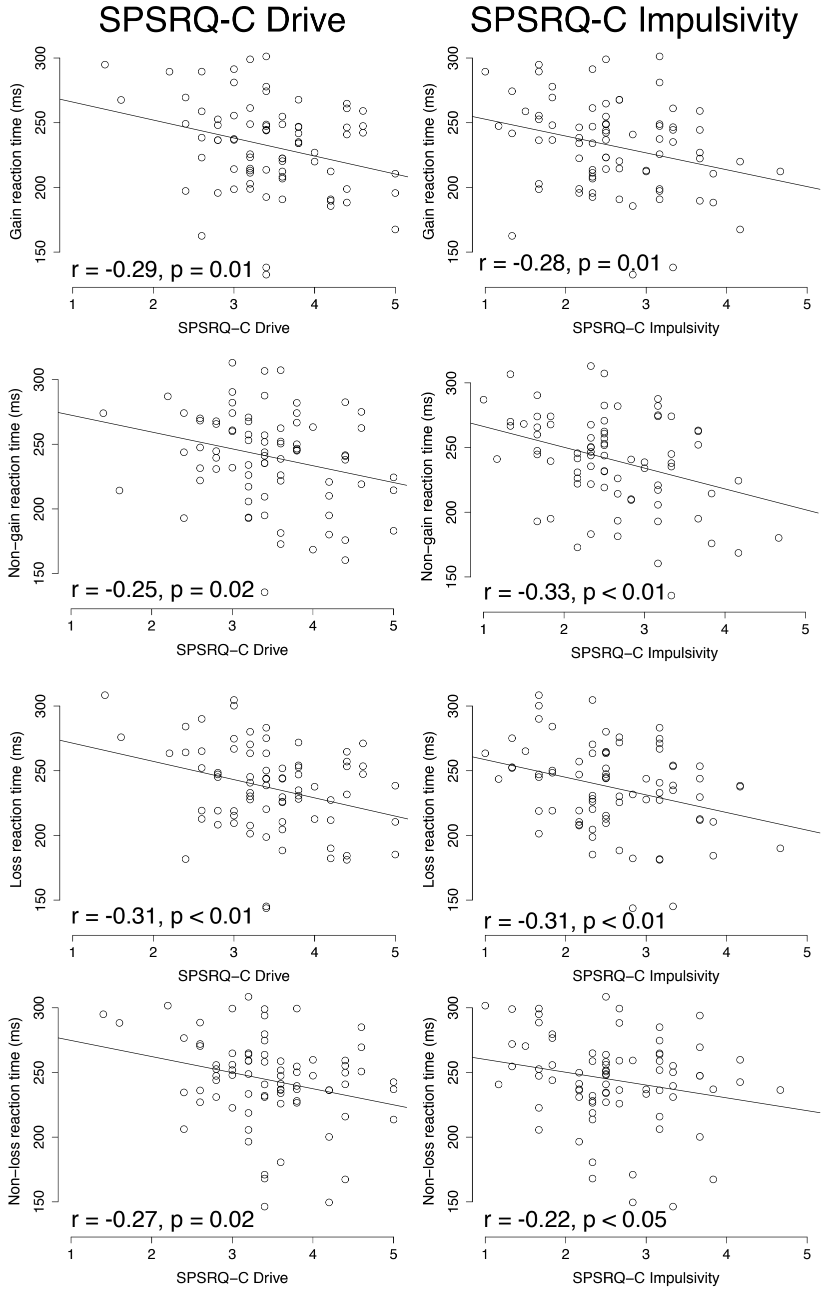

Greater self-report drive and impulsivity on the sensitivity to punishment and sensitivity to reward questionnaire for children (SPSRQ-C) was associated with faster reaction times for all incentive conditions in the KIDMID task. The reported associations are consistent with the original publication of the SPSRQ-C (Colder et al., 2011). Self-reports on the remaining three subscales of the SPSRQ-C were not associated with reaction time (Fear: gain: r=-0.16, p=0.17; non-gain: r=-0.14, p=0.23; loss: r=-0.19, p=0.09; non-loss: r=-0.12, p=0.28; Anxiety: gain: r=0.12, p=0.27; non-gain: r=0.15, p=0.18; loss: r=0.07, p=0.57; non-loss: r=0.02, p=0.88; Social approval: gain: r=-0.10, p=0.40; non-gain: r=-0.10, p=0.40; loss: r=-0.15, p=0.20; non-loss: r=-0.12, p=0.29.

Supplementary Figure 2. Whole-brain contrasts for loss versus non-loss anticipation and outcome.

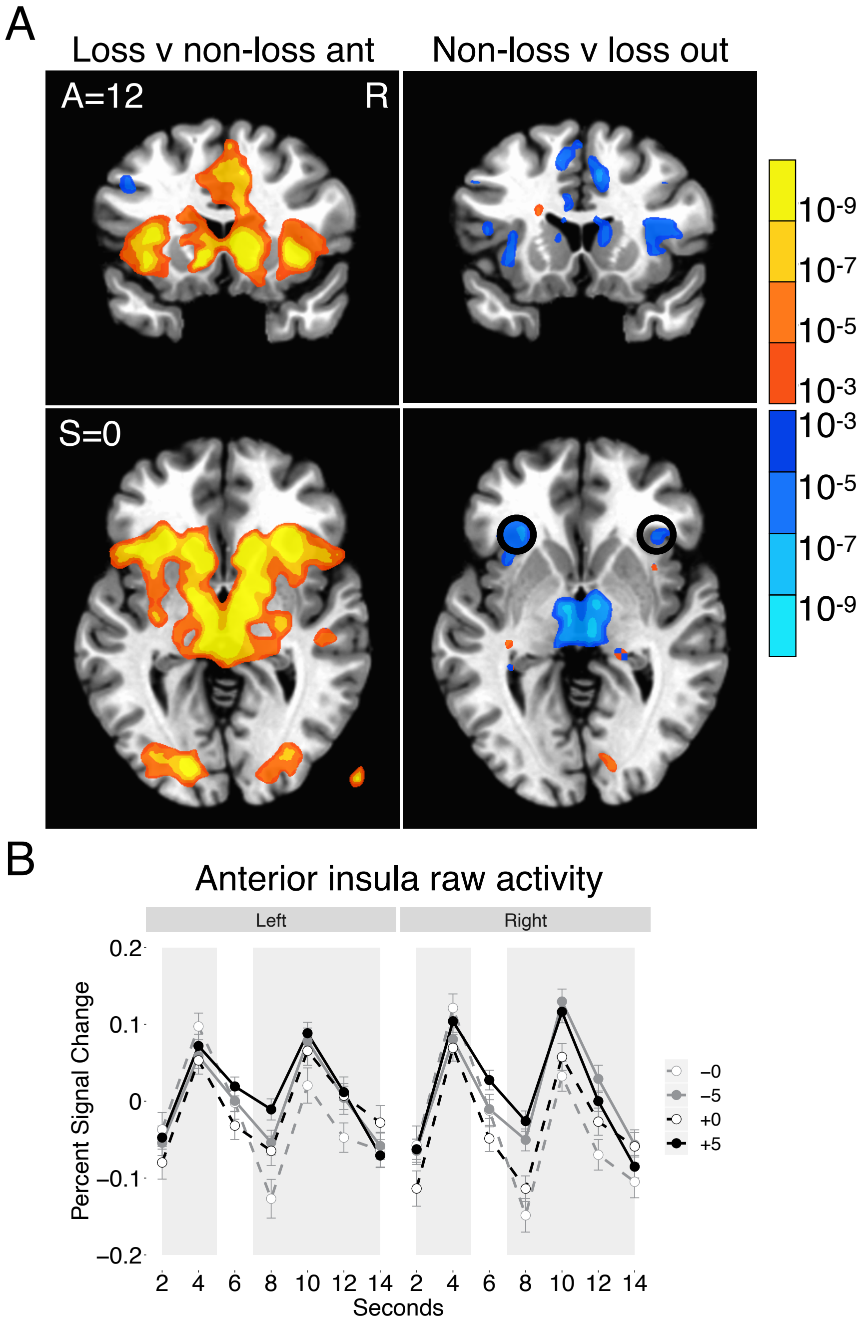

(A) Whole-brain FMRI analyses revealed increased mesolimbic activity during anticipation of potential loss versus non-loss (voxelwise $p<0.001$, cluster-corrected $p<0.05$). Loss outcomes resulted in increased anterior insula activity relative to non-loss outcomes. The spherical AIns VOI demonstrates where raw activity was extracted for the analysis in B.

(B) Raw percent signal change in AIns activity was plotted to recapitulate the whole-brain visualization. AIns activity in both hemispheres was greater for loss outcomes than for non-loss outcomes (left: paired $t(90)=2.24$, $p=0.03$; right: paired $t(90)=3.95$, $p<0.001$). Right AIns activity was greater for gain outcomes than for non-gain outcomes (left: paired $t(90)=0.95$, $p=0.34$; right: paired $t(90)=2.70$, $p<0.01$).

Supplementary Figure 3. Tract visualizations in other representative participants.

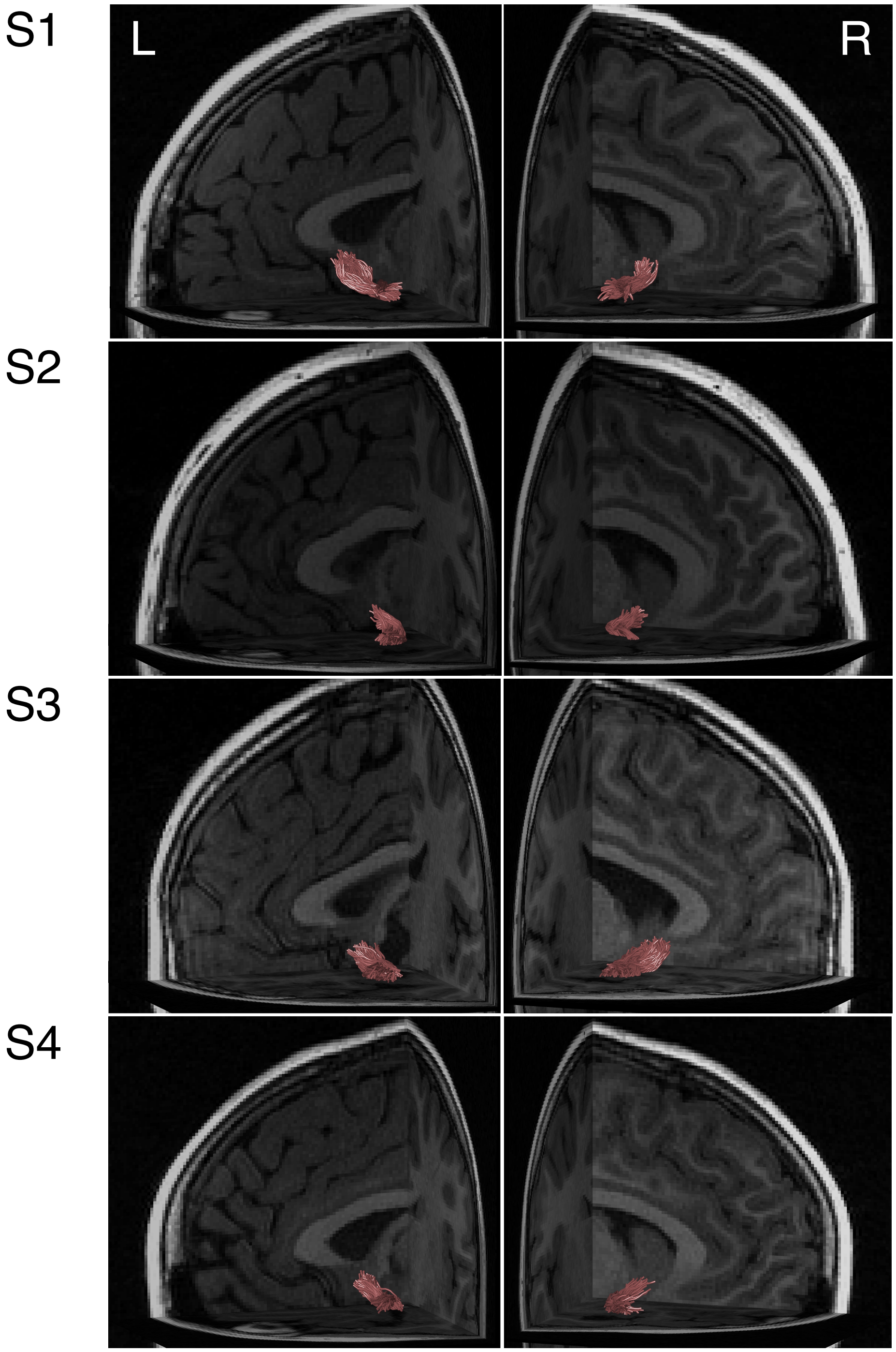

Supplementary Figure 4. Fiber Orientation Distributions generated by constrained spherical deconvolution in a representative subject.

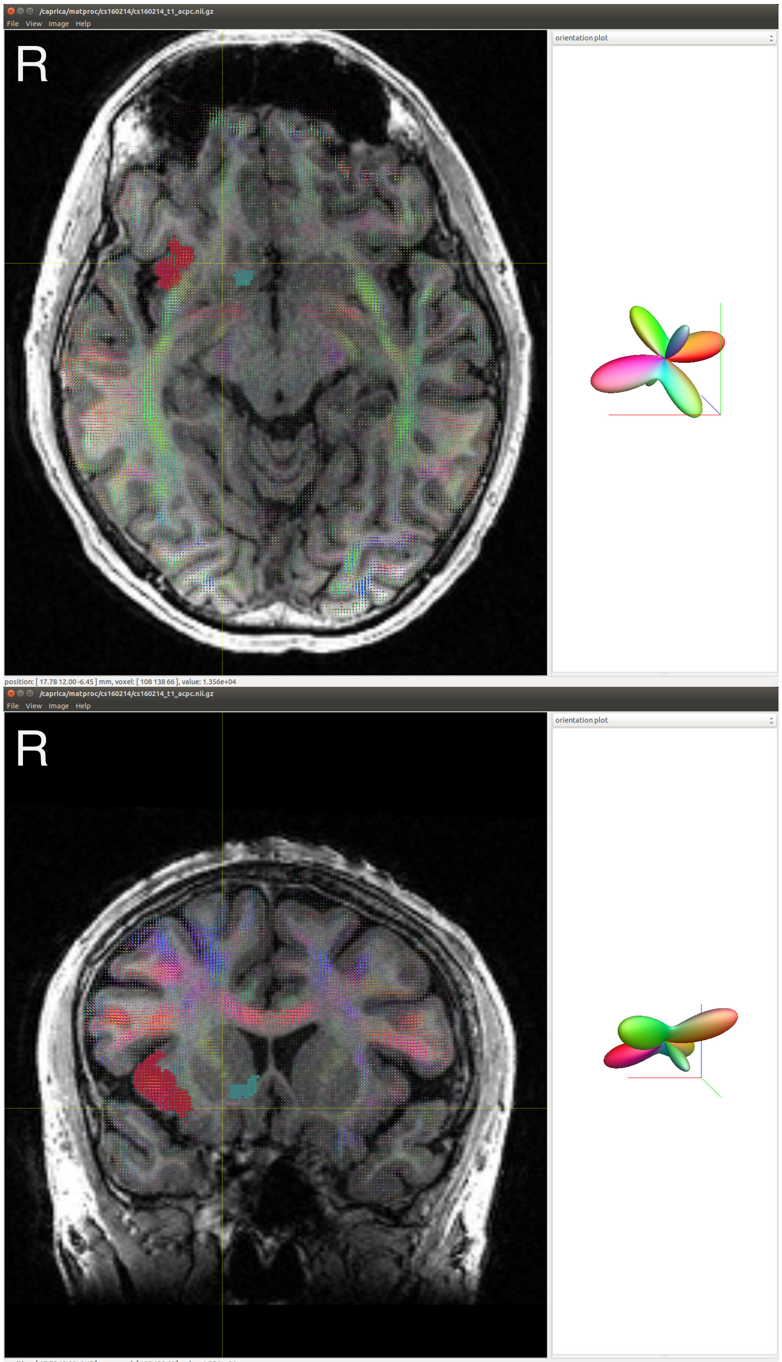

Axial and coronal views of a T1 structural image overlaid with the AIns VOI (red), the NAcc VOI (green), and the Fiber Orientation Distribution (FOD) in each voxel from constrained spherical deconvolution (lmax = 6) of the diffusion signal. A single FOD is shown for the same voxel in both views. The FOD indicates that the white matter between the AIns and NAcc follows two primary directions: (1) the longitudinal direction (green) likely indicates signal from the uncinate fasciculus, (2) the lateral direction (red) likely indicates signal from the AIns-NAcc tract.

Supplementary Figure 5. Associations between AIns-NAcc tract coherence and NAcc activity during the target and outcome task phases.

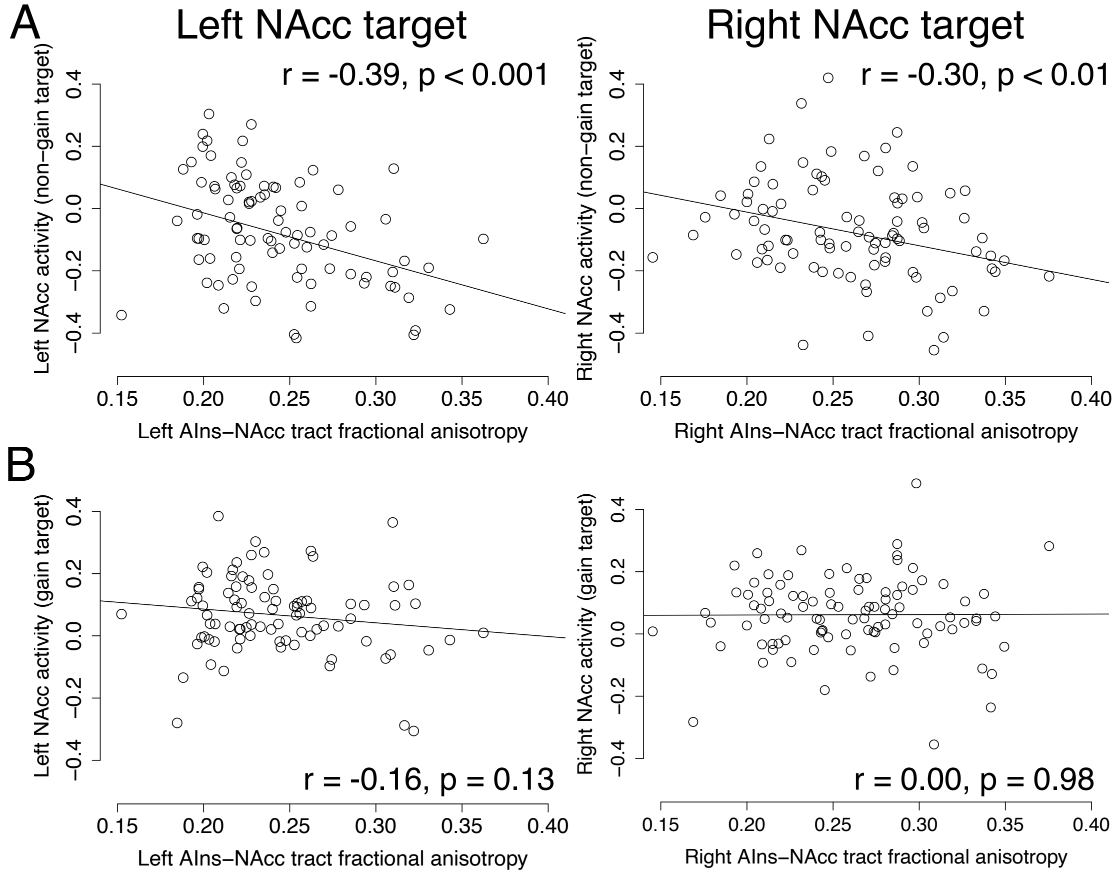

(A) Similar to anticipatory activity, AIns-NAcc tract coherence is associated with decreased NAcc activity when participants responded to targets for non-gains (right: β=-0.30, t(89)=-2.95, p<0.01; left: β=-0.39, t(89)=-4.03, p<0.001). All regression coefficients are standardized.

(B) Tract coherence was not associated with NAcc activity when participants responded to targets for gains (right: β=0.00, t(89)=-0.03, p=0.98; left: β=-0.16, t(89)=-1.53, p=0.13).

AIns-NAcc tract coherence was not associated with NAcc activity when participants viewed trial outcomes for gains and non-gains (right: β=0.13, t(89)=1.26, p=0.21; left: β=0.05, t(89)=0.46, p=0.65).

With respect to loss incentives, AIns-NAcc tract coherence was associated with greater NAcc activity during anticipation of losses (right: β=0.26, t(89)=2.54, p=0.01; left: β=0.21, t(89)=1.99, p=0.05). However, tract coherence was not associated with NAcc activity during anticipation of non-losses (right: β=-0.09, t(89)=-0.86, p=0.93; left: β=0.00, t(89)=0.01, p=0.99).

Supplementary Table 1. AIns-NAcc tract coherence is not associated with other subscales of the SPSRQ-C.

	Baseline	Follow-up
Anxiety	β=-0.20, t=-1.53, p=0.13	β=-0.03, t=-0.21, p=0.83
Fear	β=0.09, t=0.68, p=0.50	β=-0.08, t=-0.66, p=0.52
Social approval	β=0.18, t=1.52, p=0.13	β=-0.03, t=-0.28, p=0.78